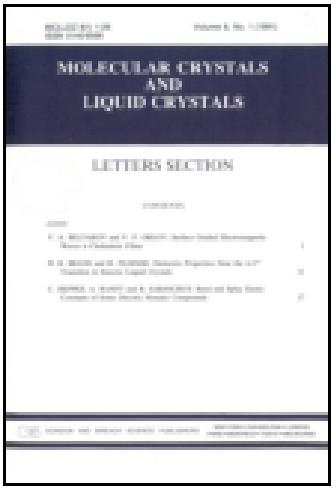

Molecular Crystals and Liquid Crystals
Publication details, including instructions for authors and subscription information:
http://www.tandfonline.com/loi/gmcl20

Quantum Chemical, Spectroscopic, and X-Ray Diffraction Studies of N-diphenylphosphino-4-methylpiperidine Selenide (1)

H. SaraÇoĞlu[a], Ö. SariÖz[b] & S. ÖznergİZ[b]

[a] Department of Middle Education, Educational Faculty, Ondokuz Mayis University, Kurupelit, Samsun, Turkey

[b] Department of Chemistry, Faculty of Science and Arts, Nigde University, Nigde, Turkey

Published online: 08 Apr 2014.

To cite this article: H. SaraÇoĞlu, Ö. SariÖz & S. ÖznergİZ (2014) Quantum Chemical, Spectroscopic, and X-Ray Diffraction Studies of N-diphenylphosphino-4-methylpiperidine Selenide (1), Molecular Crystals and Liquid Crystals, 591:1, 47-63, DOI: 10.1080/15421406.2013.822302

To link to this article: http://dx.doi.org/10.1080/15421406.2013.822302

Mol. Cryst. Liq. Cryst., Vol. 591: pp. 47–63, 2014

ISSN: 1542-1406 print/1563-5287 online
DOI: 10.1080/15421406.2013.822302

Taylor & Francis
Taylor & Francis Group

Quantum Chemical, Spectroscopic, and X-Ray Diffraction Studies of N-diphenylphosphino-4-methylpiperidine Selenide (1)

H. SARAÇOĞLU,[1,*] Ö. SARIÖZ,[2] AND S. ÖZNERGİZ[2]

[1]Department of Middle Education, Educational Faculty, Ondokuz Mayis University, Kurupelit, Samsun, Turkey
[2]Department of Chemistry, Faculty of Science and Arts, Nigde University, Nigde, Turkey

The title molecule, N-diphenylphosphino-4-methylpiperidine selenide(1), was prepared and characterized by elemental analysis, ^{1}H-NMR, ^{31}P-{^{1}H} NMR, IR, and X-ray single-crystal determination. The compound crystallizes in the monoclinic space group P $2_1/c$. In addition to the molecular geometry from X-ray determination, vibrational frequencies and gauge, including atomic orbital (GIAO) ^{1}H- and ^{31}P-{^{1}H} NMR chemical shift values of the title compound (1) in the ground state, were calculated using the Hartree–Fock and density functional methods with the 6-31G(d, p) basis set. The calculated results show that the optimized geometries can well reproduce the crystal structures. Besides, the theoretical vibrational frequencies and chemical shift values show good agreement with experimental values. The predicted nonlinear optical (NLO) properties of the title compound are greater than those of urea. In addition, density functional theory (DFT) calculations of the molecular electrostatic potentials (MEPs), frontier molecular orbitals (FMOs) of the title compound were carried out at the B3LYP/6-31G(d) level of theory.

[Supplementary materials are available for this article. Go to the publisher's online edition of Molecular Crystals and Liquid Crystals for the following free supplemental: Crystallographic data for the structural analysis have been deposited with the Cambridge Crystallographic Data Centre, CCDC No 844574. Copy of this information may be obtained free of charge from the Director, CCDC, 12 Union Road, Cambridge CB2 1EZ, UK (fax: +44-1223-336033; e-mail: deposit@ccdc.cam.ac.uk or www: http://www.ccdc.cam.ac.uk).]

Keywords Aminophosphines; chalcogenides; computational chemistry; NMR spectroscopy; X-ray structure determination

Introduction

Aminophosphines are tricoordinate phosphorus compounds containing one to three polar and labile P(III)–N, bonds and they are considered as one of the most intriguing in chemistry [1]. Aminophosphines and their derivatives play an important role in the fight

*Address correspondence to H. Saraçoğlu, Department of Middle Education, Educational Faculty, Ondokuz Mayis University, 55139 Kurupelit, Samsun, Turkey. Tel.: +90 362 457 60 77; Fax: +90 362 4576078. E-mail: hanifesa@omu.edu.tr

against cancer, as part of catalytic systems in industrially important reactions, as well as herbicidal, neuroactive, and antimicrobial agents [2]. In addition, they have shown promising application potential in some electronic devices. More importantly, aminophosphines have also started serving as effective ligands in synthesizing a variety of metal complexes which in turn have found applications as catalysts in a real huge variety of organic reactions and conversions [3]. The design of highly active and selective catalysts is becoming more and more important in the study of catalytic processes, such as hydroformylation of alkenes. An extensive study has been carried out on the steric and electronic properties of the ligands [4] Aminophosphines are one of the most important ligands in catalysis because they allow the tuning of catalysts in terms of steric and electronic effects. The fact that the donor and acceptor properties of P(III) compounds are easily tuned by changing the nature of the substituents on the phosphorus atom or nitrogen atom makes them good examples for developing their coordination behavior with transition metal substrates [3, 5]. Therefore, varying substituents on the nitrogen offers scope for maneuvering the aminophosphine ligands to best suit for a specific catalytic application. Aminophosphines undergo oxidative addition reactions with chalcogens/chalcogen sources to give the corresponding aminophosphine chalcogenide, which themselves possess ligating behavior, and hence they find applications in catalysis, besides being used as carriers of Group 16 elements in electronic industries, and they are more stable compared with the corresponding free aminophosphines [1, 6–8]. Characterization of phosphine selenides also provides an insight into electronic properties of phosphine ligands. The value of the $^{1}J_{PSe}$ coupling constant in phosphine selenides can be correlated with the electron donating or electron withdrawing properties of the phosphines [9].

This has prompted us to extend our studies on the synthesis and solid-state structure of new aminophosphine selenide derivative, which might be useful for transition metal chemistry and catalytic applications. As a part of our research program on this subject, we present results of a detailed investigation of the synthesis and structural characterization of N-diphenylphosphino-4-methylpiperidine selenide (1) by using single crystal X-ray, IR, ^{1}H-NMR, and ^{31}P-$\{^{1}H\}$ NMR. The vibrational assignments of the title compounds (1) in the ground state have been calculated by using the Hartree-Fock (HF)/6-31G(*d*, *p*) and DFT(B3LYP)/6-31G(*d*, *p*) method. The structural geometry, molecular electrostatic potential (MEP), frontier molecular orbitals (FMO), and nonlinear optical (NLO) properties of the title compound were studied at the B3LYP/6-31G(*d*) level. A comparison of the experimental and theoretical spectra can be very useful in making correct assignments and understanding the basic chemical shift molecular structure relationship. And so, these calculations allow a precise description of the properties of phosphine ligands and a priori modeling of new phosphines with desired properties.

Experimental

General

Reactions were routinely carried out using Schlenk-line techniques under pure dry nitrogen gas. Solvents were dried and distilled prior to use. All other chemicals were reagent grade, available commercially and used without further purification. Melting points were determined on an Electrothermal A 9100 and are uncorrected. ^{31}P-$\{^{1}H\}$ and ^{1}H NMR spectra were taken on Bruker UltraShield-400 spectrophotometer. Infrared spectra were recorded on a Perkin Elmer FT-IR System Spectrum BX. Elemental analysis was performed in a TruSpec Micro.

Synthesis of Aminophosphine Chalcogenide

Preparation of $PPh_2NC_5H_9CH_3$. Triethylamine (3.8 mL, 27.41 mmol) and Ph_2PCl (5.0 mL, 27.19 mmol) were sequentially added with stirring to a solution of 4-methylpiperidine (3.2 mL, 27.10 mmol) in tetrahyrofuran (THF) (20 mL). The reaction mixture was stirred for 6 h and then filtered to remove $Et_3N.HCl$. The resulting solution was evaporated under reduced pressure and the product dissolved with diethyl ether in an acetone–dry ice bath. The mixture was allowed to warm slowly at room temperature. The solvent was removed under vacuum to give a white solid of the crude product, which was crystallized from CH_2Cl_2/diethyl ether mixture (2:1) at 0°C. Yield 6.30 g (82%). m.p.: 158°C. Elemental Analysis: $C_{18}H_{22}PN$ (283.35 g mol^{-1}) Found (Required): C, 76.18 (76.30); H, 7.62 (7.83); N, 4.66 (4.94).

Preparation of $Ph_2P(Se)NC_5H_9CH_3$ (1). A mixture of $PPh_2NC_5H_9CH_3$ (0.526 g, 1.85 mmol) and grey Se (0.15 g, 1.90 mmol) in toluene (20 mL) was heated under reflux for 3 h to give a clear solution. Ligand 1 (0.526 g, 1.85 mmol) and grey Se (0.15 g, 1.90 mmol) were refluxed in toluene (20 mL) for 3 h. The reaction mixture was concentrated to ca. 1–2 mL in vacuo and diethylether (20 mL) was added. The precipitate was filtered and dried in air to yield 1. Yield 0.42 g (63%). m.p.: 133°C. Elemental Analysis: $C_{18}H_{22}PNSe$ (362.31 g mol^{-1}) Found (Required): C, 59.55 (59.67); H, 6.04 (6.12); N, 3.68 (3.87).

Crystallography

The data collection was performed at 296 K on a Stoe-IPDS-2 diffractometer equipped with a graphite monochromated Mo-K_α radiation ($\lambda = 0.71073$ Å). The structure was solved by direct methods using SHELXS-97 and refined by a full-matrix least-squares procedure using the program SHELXL-97 [10]. All nonhydrogen atoms were easily found from the different Fourier maps and refined anisotropically. All hydrogen atoms were included using a riding model and refined isotropically with CH = 0.93 (for phenyl groups), $CH_2 = 0.97$, $CH_3 = 0.96$, CH = 0.98 Å. $U_{iso}(H) = 1.2\ U_{eq}$ (1.5 U_{eq} for methyl group). Details of the data collection conditions and the parameters of the refinement process are given in Table 1.

Theoretical Calculations

The molecular structure of the title compound (1) in the ground state (in vacuo) was optimized by HF/6-31G(*d*, *p*) method and B3LYP method with 6-31G(*d*), 6-31G(*d*, *p*) basis sets. For the modeling, the initial guess of the title compound (1) was first obtained from the X-ray coordinates. Then, vibrational frequencies for optimized molecular structure with HF/6-31G(*d*, *p*) and B3LYP/6-31G(*d*, *p*) methods were calculated and scaled by 0.9181 and 0.9806 [11], respectively. The geometry of the title compound (1), together with those of tetramethylsilane (TMS) and phosphoric acid (H_3PO_4), was fully optimized. ^{1}H- and ^{31}P-{^{1}H} NMR chemical shifts were calculated within GIAO approach [12, 13] applying B3LYP and HF methods [14] with 6–31G(*d*, *p*) basis set.

To investigate the reactive sites of the title compound, the MEP was evaluated using the B3LYP/6-31G(*d*) method. MEP, V(*r*), at a given point *r* (*x*, *y*, *z*) in the vicinity of the molecule is defined in terms of the interaction energy between the electrical charge generated by the molecule's electrons and nuclei and a positive test charge (a proton) located at *r*. For the system studied, the $V(r)$ values were calculated as described previously

Table 1. Crystallographic data for the title compound (1)

Empirical formula	C_{18} H_{22} N P Se
Molecular weight	362.30
Temperature, T (K)	296
Wavelength (Å)	0.71073
Crystal system	monoclinic
Space group	P 2_1/c
a (Å)	10.6014 (3)
b (Å)	13.7441 (4)
c (Å)	12.2003 (4)
β (°)	93.307 (3)
Volume, V (Å^3)	1774.71 (9)
Z	4
Calculated density (g cm^{-3})	1.356
μ (mm^{-1})	2.200
F(000)	744
Crystal size(mm)	0.800 × 0.457 × 0.250
Θ range(°)	1.9/27.6
Index range (h, k, l)	−13/13, −17/17, −15/15
Reflections collected	29075
Independent reflections (R_{int})	4087 (0.115)
Observed reflections[$I > 2\sigma(I)$]	3383
Data/parameters	4087/190
Goodness-of-fit on F^2	1.09
Final R indices [$I > 2\sigma(I)$]	0.054
wR indices [$I > 2\sigma(I)$]	0.140
Largest diff. Peak and hole (e. Å^{-3})	0.86 and −0.48

using the equation [15]

$$V(r) = \sum \frac{Z_A}{|R_A - r|} - \int \frac{\rho\left(r'\right)}{|r' - r|} \mathrm{d}^3 r' \tag{1}$$

where Z_A is the charge of nucleus A, located at R_A, $\rho\left(r'\right)$ is the electronic density function of the molecule, and $r\prime$ is the dummy integration variable. The mean linear polarizability and mean first hyperpolarizability properties of the title compound were obtained from molecular polarizabilities based on theoretical calculations. All the calculations were performed by using Gauss–View molecular visualization program [16] and Gaussian 03 program package [17] on personal computer without specifying any symmetry for the title molecule (1).

Results and Discussion

Although many synthetic methods like condensation, scrambling, and transamination reactions are reported in the literature, the condensation route is the most widely used and the best one for synthesizing a wide variety of P(III)–N compounds [1]. The reaction of

4-methylpiperidine with diphenylchlorophosphine affords the corresponding aminophosphine. Oxidation of $PPh_2NC_5H_9CH_3$ by grey selenium gave the corresponding selenide (1). The synthesis of aminophosphine chalcogenide is shown in Scheme 1.

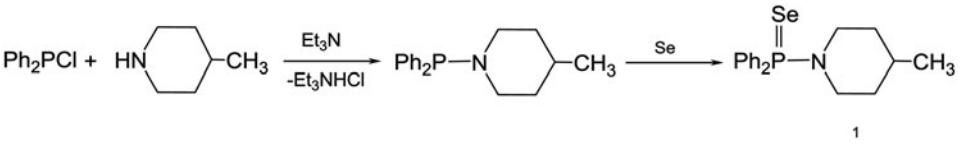

Scheme 1. Synthesis of N-diphenylphosphino-4-methylpiperidine selenide (I).

It is interesting to note that if a ligand is strongly electron-rich, it also has a high tendency to be oxidized, thus making it highly air sensitive. Therefore, we could not obtained P=O derivative of the aminophosphine.

Crystal Structure

The compound (1) crystallizes in the monoclinic space group $P2_1/c$. Details of crystal parameters, data collection, structure solution, and refinement are given in Table 1. The structure of the title compound (1) is shown in Fig. 1 [18].

The title compound (1) contains two phenyl rings and a methylpiperidine ring. The two phenyl rings are planar with maximum deviations of 0.0064(25) and 0.0075(30) Å, respectively. The dihedral angles among the 4-methylpiperidine plane A (N1/C13-C17), the phenyl plane B (C1–C6), and the other phenyl plane C (C7–C12) are 51.28 (12)° (A/B), 60.13 (12)° (A/C), and 80.32 (10)° (B/C).

The P−N bond length of 1.66 Å is shorter than the normally accepted value for a single bond (1.77 Å) [19]. The P=Se bond length, 2.1071(7) Å, agree with well literature values [20–22]. In fact, variations in P=Se bond length values elucidated from X-ray crystallography in such selenide compounds are generally attributed to the various extent of contribution of dipolar and π-bond structures [1]. Studies led to the conclusion that the dipolar form is important for E = S and Se. This was supported by dipole moment studies carried out for P=E and was found that the polarity of the molecule increases with the increase in the atomic size: O < S < Se [1]. P=Se bond distances are observed in the range 2.04–2.11 Å. There is a correlation between the electronic nature of the substituents and the P–Se distance, with electron donating groups leading to larger bond lengths than electron withdrawing groups. The P=Se bond length is longer than average P=Se bond length. This can be understood on the basis of the two resonance forms $R_3P{=}Se$ and $R_3P^+–Se^-$. The P–Se bond length (2.1071 Å) is a consequence of the greater contribution of the $R_3P^+–Se^-$ resonance form. The ionic resonance form is stabilized by electron donating substituents [9]. The P=Se bond distance shows that $Ph_2PNC_5H_9CH_3$ is strong σ-donor.

The 4-methylpiperidine ring is in a chair conformation, as indicated by the Cremer and Pople puckering parameters (Q = 0.590(3) Å, ϕ = 348(5)°, and θ = 3.1(3)°) [23]. The phosphorus centre, coordinated by two phenyl rings and the 4-methylpiperidine ring (P−C−C−C), adopts an antiperiplanar conformation. The PNC_2Se coordination forms a slightly distorted tetrahedral geometry, the angles around the P atom ranging form 103.1(12) to 117.23(9)°. The bond lengths and angles in (1) are shown in Table 2.

Within the title compound (1), there are two intra-molecular C−H · Se hydrogen bonds (Table 3), with the Se atom acting as an acceptor in the formation of two S(5) motif [24]. In crystal packing, no classical hydrogen bond is found. The C5 atom of phenyl ring (B)

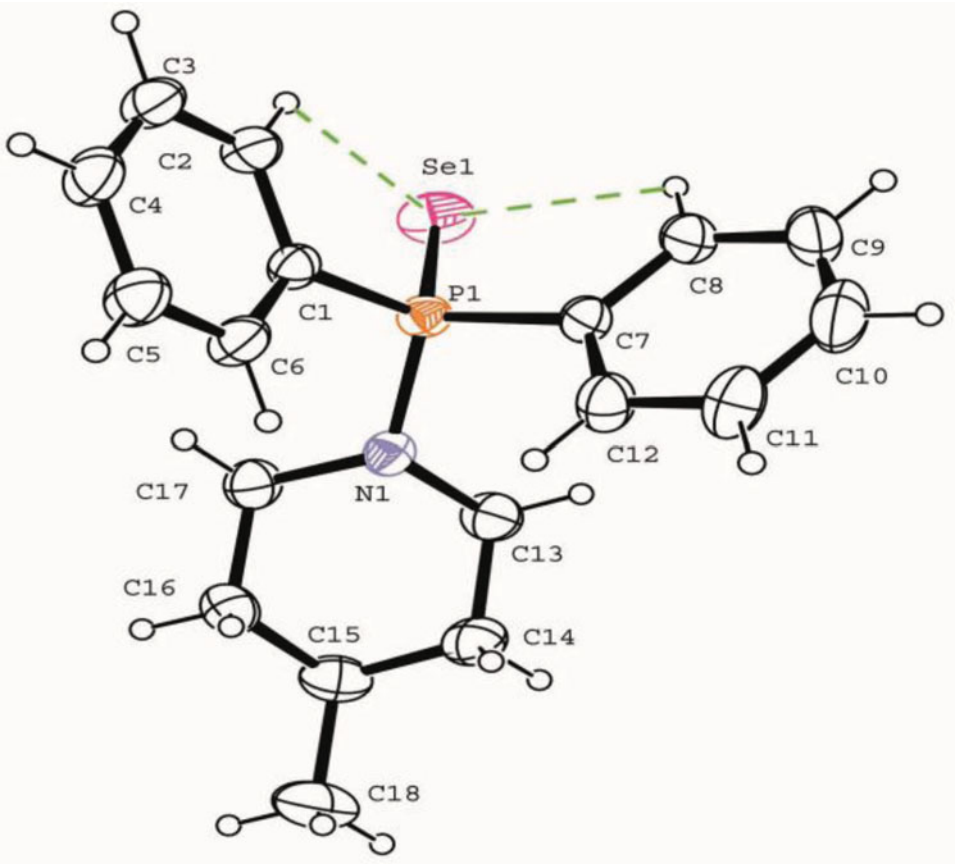

Figure 1. Ortep III diagram of the title compound (1). Displacement ellipsoids are drawn at the 30% probability level and H atoms are shown as small spheres of arbitrary radii.

in the molecule (1) at (x, y, z) acts as a hydrogen-bond donor, via atom H5, to the phenyl ring (C) at (x, 1/2 – y, –1/2 + z), linking the chain along the c axis, as shown in Fig. 2. In addition, there is intermolecular $\pi \cdot \pi$ interaction between the phenyl rings. Dipole–dipole and van der Waals interactions are also effective in the molecular packing in the crystal structure (1).

Optimized Structure (1)

Theoretically calculations were performed on the title compound ($Ph_2P(Se)NC_5H_9CH_3$) at HF/6-31G(d, p), B3LYP/6-31G(d), and B3LYP/6-31G(d, p) levels. Some optimized geometric parameters are also listed in Table 2. Using the root mean square error (RMSE) for evaluation, HF/6-31G(d, p) is the ab initio calculation that the best predicts the bond distances. DFT/6-31G(d) calculation provides the lowest RMSE for bond angles (0.921°).

The dihedral angles between optimized counterparts of the title compound (1) are calculated at 61.42° (A/B), 61.42° (A/C), and 73.52° (B/C) for HF/6-31G(d, p), at 63.88° (A/B), 63.92° (A/C), and 72.72° (B/C) for B3LYP/6-31G(d), at 63.95° (A/B), 63.98° (A/C), and 72.67° (B/C) for B3LYP/6-31G(d, p).

Table 2. Selected theoretical and experimental geometric parameters in the title compound (1) (bond lengths in Å, bond angles in degrees)

	Experimental	HF 6-31 (*d*, *p*)	B3LYP 6-31 (*d*)	B3LYP 6-31 (*d*, *p*)
Bond lengths (Å)				
P–Se	2.1071(7)	2.109	2.114	2.113
P═N	1.663(2)	1.690	1.721	1.720
P–C7	1.816(3)	1.828	1.840	1.839
N–C13	1.476(4)	1.473	1.483	1.483
C15–C18	1.529(5)	1.528	1.532	1.531
RMSE[a]		0.013	0.028	0.028
Max. difference[a]		0.027	0.058	0.057
Bond Angles (°)				
Se–P═N	117.23(9)	115.77	117.48	117.42
Se–P–C1	113.88(9)	113.00	113.09	113.07
Se–P–C7	113.23(9)	113.00	113.08	113.07
C1–P–C7	103.65(12)	105.49	105.50	105.55
N1–P–C7	103.01(12)	104.27	103.19	103.21
N1–P–C1	104.33(11)	104.28	103.19	103.21
C16–C15–C18	111.5(3)	112.03	112.19	112.20
RMSE[a]		1.083	0.921	0.934
Max. difference[a]		1.840	1.850	1.900
Dihedral angles (°)				
C2–C1–P–Se	−23.0(3)	−14.81	−13.62	−13.67
C6–C1–P–Se	161.9(2)	167.27	168.43	168.36
C13–N–P–Se	65.0(2)	65.45	64.16	64.11
C17–N–P–Se	−70.7(2)	−65.48	−64.12	−64.07
C8–C7–P═N	142.6(2)	141.37	141.48	141.50

[a]RMSE and maximum differences between the bond lengths and the bond angles computed by the theoretical method and those obtained from X-ray diffraction.

Analyses of Vibrational Spectra of (1)

FT-IR spectrum was recorded on a Perkin Emler FT-IR System Spectrum BX as KBr pellets. Harmonic vibrational frequencies of the title compound (1) were calculated by using HF

Table 3. Hydrogen bond geometries in crystal structure 1 (Å, °)

D–H · A	D–H (Å)	H · A (Å)	D · A (Å)	D–H · A(°)
C2–H2 · Se1	0.93	2.97	3.482(3)	116
C8–H8 · Se1	0.93	2.94	3.457(3)	117
C5–H5 · Cg3[i]	0.93	2.98	3.619(4)	127

Cg3 is the centroid of the C ring.
Symmetry code: (i): x, 1/2 – y, –1/2 + z.

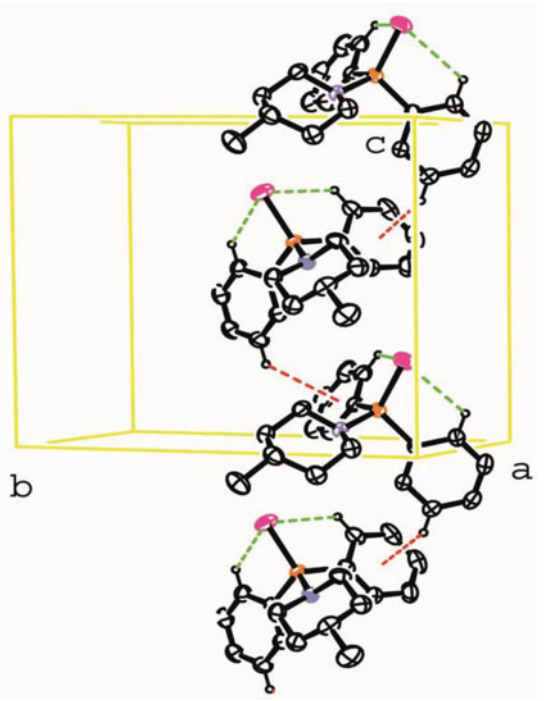

Figure 2. A partial packing diagram for the compound (1), showing the C−H · π interactions as broken lines. Hydrogen atoms not involved in hydrogen bonding have been omitted. [Symmetry code: x, 1/2 – y, –1/2 + z].

and DFT methods with 6-31G(d, p) basis set, and the obtained frequencies were scaled by 0.9181 and 0.9806 [11]. In order to facilitate assignment of the observed peaks, we have analyzed vibrational frequencies and compared our calculation of the title compound (1) with their experimental results and shown in Table 4.

The aromatic structure shows the presence of C−H stretching vibrations in the region 2900–3150 cm^{-1} which is the characteristic region for the ready identification of the C−H stretching vibrations [25,26]. In this molecule, experimentally C−H stretching vibration of the title compound (1) is observed at 2946 cm^{-1}, while it has been calculated at 3092 cm^{-1} for HF and 3142 cm^{-1} for B3LYP. The vibrations in this region (2900–3150 cm^{-1}) are in agreement with experimental assignment. The experimental P−N and P=Se stretch modes were observed at 933 and 516 cm^{-1}, which have been calculated with HF and DFT methods at 925–550 cm^{-1} and 903–545 cm^{-1}, respectively. The P=Se stretch mode agrees with well literature value [27]. The other calculated vibrational frequencies can be seen in Table 4. In general, when the calculated IR frequencies are compared with the experimental data of the title compound, all these data agree with calculated vibrations.

^{1}H and ^{31}P-{^{1}H} NMR Spectra of the Title Compound (1)

DFT and HF methods differ in that no electron correlation effects are taken into account in HF. DFT methods treat the electronic energy as a function of the electron density of all electrons simultaneously and thus include electron correlation effect [28]. GIAO ^{1}H and ^{31}P-{^{1}H} chemical shift values (with respect to TMS and H_3PO_4, respectively) were

Table 4. Comparison of the observed and calculated vibrational spectra of the title compound (1)

Assignments	Experimental	HF 6-31G (*d*, *p*)	B3LYP 6-31G (*d*, *p*)
ν_s C−H (aromatic)		3111	3155
ν_s C−H (aromatic)		3110	3149
ν_s C−H (aromatic)		3093	3144
ν_s C−H (aromatic)	2946	3092	3142
ν_{as} C−H (aromatic)		3081	3133
ν_{as} C−H (aromatic)		—	3126
ν_s C−H_2 (aromatic)		3018	3056
ν_{as} C−H_2(aromatic)		3016	3055
ν_{as} C−H_3		2977	3048
ν_{as} C−H_3	2844	2975	3042
ν_{as} C—H_2 (aromatic)		—	3017
ν_{as} C−H_2 (aromatic)		—	3014
ν_s C−H_3 + ν_s C−H_2 (aromatic)		2958	2977
ν_s C−H_2 (aromatic)		2954	2968
ν_s C−H_2 (aromatic) + ν_s C−H_3		2921	—
ν_s C−H_2 (aromatic)		2917	—
ν_s C−H_2 (aromatic)		2915	—
ν C−H (aromatic) + ν_s C−H_2 (aromatic)		—	2945
ν C−H (aromatic) + ν_s C−H_2 (aromatic)		—	2937
ν_s C−H_3		2912	—
ν_s C−H_2 (aromatic)		2911	2935
γ CH (aromatic)	1476	1517	—
γ CH (aromatic)	1438	1466	1451
γ CH_2 (aromatic)	1371	1433	1391
γ CH (aromatic)		1351	—
α CH_2 (aromatic)	1311	1273	1249
α CH (aromatic)	1242	—	1188
α CH_2 (aromatic)	1178	1198	1182
α CH (aromatic)		1195	—
γ CH_2 (aromatic)		1178	—
β CH_2 (aromatic)		1171	—
γ CH (aromatic)		—	1094
ν C−C (aromatic)		1123	1093
α CH (aromatic)		1115	—
ν P−C	1097	1108	1091
α CH (aromatic)		1106	1083
ω CH_2 (aromatic)		1097	—
α CH_2 (aromatic)	1052	1055	1036
β CH (aromatic)+ ω CH_2 (aromatic)		956	—

(Continued on next page)

Table 4. Comparison of the observed and calculated vibrational spectra of the title compound (1) *(Continued)*

Assignments	Experimental	HF 6-31G (*d*, *p*)	B3LYP 6-31G (*d*, *p*)
ν P—N	933	925	903
ω CH (aromatic)	788	785	758
ω CH_2 (aromatic)		781	—
ω CH (aromatic)	758	774	748
ω CH_2 (aromatic)	743	727	713
θ (aromatic)	720	715	705
ω CH (aromatic)	710	713	701
θ (aromatic)	694	703	696
ω CH_2 (aromatic)		569	567
ν P═Se	516	550	545
δ CH (aromatic)	504	522	514
δ CH (aromatic)	498	505	—
δ CH (aromatic)	480	444	—

Vibrational modes: ν, stretching; β, bending; α, scissoring; γ, rocking; ω, wagging; δ, twisting; θ, ring breathing; *s*, symmetric; as, asymmetric.

calculated using the HF and B3LYP methods with 6-31G(d, p) basis set and compared with experimental ^{1}H and ^{31}P-$\{^1H\}$ chemical shift values. The results of these calculations are shown in Table 5.

The signals in the range 1.29–2.96 ppm were assigned to C(13)H_2, C(14)H_2, C(16)H_2, and C(17)H_2 protons, and were calculated at 1.13–2.41 ppm for HF/6-31G(d, p) and 1.34–2.79 ppm for B3LYP/6-31G(d, p). The C—H signal of the 4-methylpiperidine ring was observed at 1.54 ppm. The phenyl protons were observed at 7.47 ppm and 8.09 ppm. ^{31}P-$\{^1H\}$ NMR spectrum of the compound (1) shows the signal at 68.1 ppm. The signal has been calculated as 98.46 ppm for HF level, 109.32 ppm for B3LYP level. Table 5 shows the other calculated chemical shift values. As can be seen from Table 5, calculated ^{1}H and ^{31}P-$\{^1H\}$ chemical shift values of the title compound (1) are agreement with the experimental ^{1}H and ^{31}P-$\{^1H\}$ shift data.

The ^{31} P-$\{1H\}$ NMR spectrum of compound (1) consists of singlet with ^{77}Se satellites and the coupling constant value ($^1J_{PSe}$) is 750.58 Hz. The coupling constant value ($^1J_{PSe}$), which varies over a wide range depending upon the nature of substituents on phosphorus, is so useful that the basicity of phosphines was determined based on ^{31}P-$\{^1H\}$ NMR. There is a good established correlation between $^1J_{PSe}$ and the electronic properties of the parent phosphorus ligands, which takes the form of an inverse relationship with the σ-basicity [9]. The value of the $^1J_{PSe}$ coupling constant for 1 ($^1J_{PSe}$ = 750.58 Hz) is significantly smaller than for the aminophosphine selenides derived from piperazine which we reported earlier [7] ($Ph_2P(Se)NC_4H_8NC_6H_5$, $^1J_{PSe}$ = 773.80 Hz; $Ph_2P(Se)NC_4H_8NC_6H_5$, $^1J_{PSe}$ = 765.60 Hz), suggesting that $Ph_2PNC_5H_9CH_3$ is a strong σ-donor and the electron withdrawing of 4-methypiperidine group attached to phosphorus is low. The value of the coupling constant ($^1J_{PSe}$ = 750.58 Hz) of $Ph_2P(Se)NC_5H_9CH_3$ shows that $Ph_2PNC_5H_9CH_3$ is a strong σ-donor and the electron withdrawing of 4-methypiperidine group attached to phosphorus is

Table 5. Theorical and experimental ^{31}P and ^{1}H isotropic chemical shifts (with respect to H_3PO_4 and TMS all values in ppm) for the title compound (1)

Atom	Experimental (ppm) $CDCl_3$	Calculated chemical shift (ppm)	
		HF	B3LYP
P	68.1	98.46	109.32
H2	8.09	8.96	8.65
H3	7.47	7.64	7.45
H4	7.47	7.72	7.40
H5	7.47	7.56	7.38
H6	8.09	8.46	8.31
H8	8.09	8.96	8.65
H9	7.47	7.64	7.45
H10	7.47	7.72	7.40
H11	7.47	7.56	7.38
H12	8.09	8.46	8.31
H13a	2.59	2.32	2.65
H13b	2.96	2.41	2.79
H14a	1.29	1.13	1.34
H14b	1.67	1.27	1.49
H15	1.54	1.27	1.57
H16a	1.67	1.27	1.49
H16b	1.29	1.13	1.35
H17a	2.96	2.41	2.79
H17b	2.59	2.32	2.65
H18*	0.97	0.95	0.91

*Average.

low. The new very electron-rich ligand prepared here should, given its ease of preparation, be a useful tool in organometallic chemistry and catalysis.

Two resonance forms for aminophosphine chalcogenides are known and the dipolar form is important for selenide derivatives. ^{31}P chemical shift value of the title compound (1) supports the fact that for aminophosphine selenide 1, the dipolar form P^+–E^- predominates [3]. The dipolar form is stabilized by electron donating substituents [9]. Also, the value of the coupling constant of 1 shows that $Ph_2PNC_5H_9CH_3$ is a strong σ-donor. Therefore, the P═Se bond length is longer than average P═Se bond length.

Molecular Electrostatic Potential (MEP)

The MEP is related to the electronic density and is a very useful descriptor in understanding sites of electrophilic attack and nucleophilic reactions as well as hydrogen bonding interactions [29–31]. The electrostatic potential $V(r)$ is also well suited for analyzing processes based on the "recognition" of one molecule by another, such as in drug–receptor, and enzyme–substrate interactions, because it is through their potentials that the two species first "see" each other [32, 33]. Being a real physical property, $V(r)$ can be determined experimentally by diffraction or by computational methods [34].

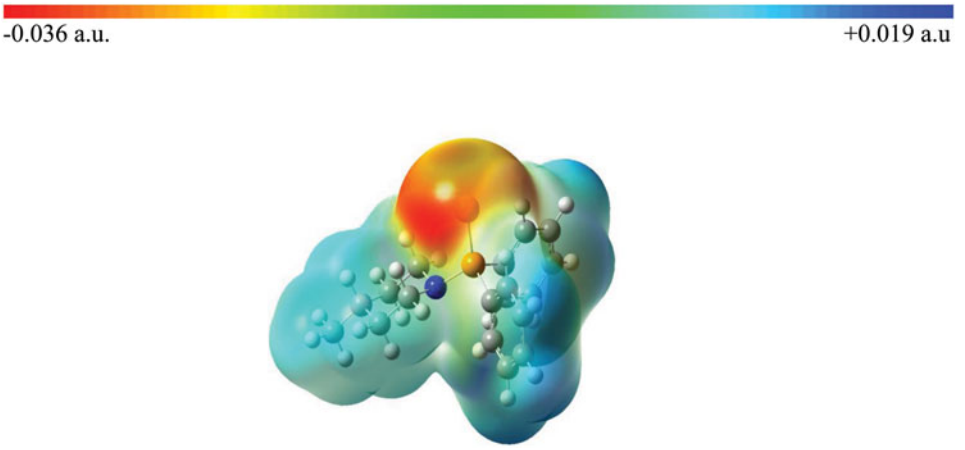

Figure 3. Molecular electrostatic potential map calculated at B3LYP/6-31G(*d*) level.

MEP was calculated by using B3LYP/6-31G(*d*) method. The red regions and blue regions of MEP represent negative and positive potentials, respectively. As can be seen in Fig. 3, this molecule has one possible site of electrophilic attack. The negative region is localized on selenium atom with minimum value of –0.036 a.u. Also, positive electrostatic potential regions are over the carbon atoms of the phenyl rings and the 4-methylpiperidine ring. The positive $V(r)$ values are about +0.019 a.u. for C15 atom, which is the most positive region, about +0.016 a.u. for C5 atom. According to these calculated results, the MEP map shows that the negative potential site is on electronegative atom as well as the positive potential sites are around the hydrogen atoms. These sites give information concerning the region from where the compound can undergo noncovalent interactions.

Frontier Molecular Orbitals

The FMOs play an important role in the electric and optical properties, as well as in UV–Vis spectra and chemical reactions [35]. Figure 4 shows the distributions and energy levels of the HOMO–1, HOMO, LUMO, and LUMO+1 orbitals computed at the B3LYP/6-31G(d) level for the title compound.

As can be seen from Fig. 4, the HOMO-1 is mainly localized on P=Se bond and N atom of the 4-methylpiperidine ring. For the HOMO, the electrons are delocalized on P=Se bond and partly delocalized over the diphenyl ring. While the electrons are delocalized over the diphenyl ring in the LUMO+1, they are delocalized over the diphenyl ring, the P=Se bond and partly delocalized over the 4-methylpiperidine ring on the LUMO. Both the HOMOs and LUMOs are mostly the π antibonding type orbitals. The energy separation between the HOMO and LUMO is 4.207 eV. This large HOMO–LUMO gap automatically means high excitation energies for many of the excited states, good stability and a large chemical hardness for the title compound.

Nonlinear Optical Effects (NLO)

NLO effects arise from the interactions of electromagnetic fields in various media to produce new fields altered in phase, frequency, amplitude, or other propagation characteristics

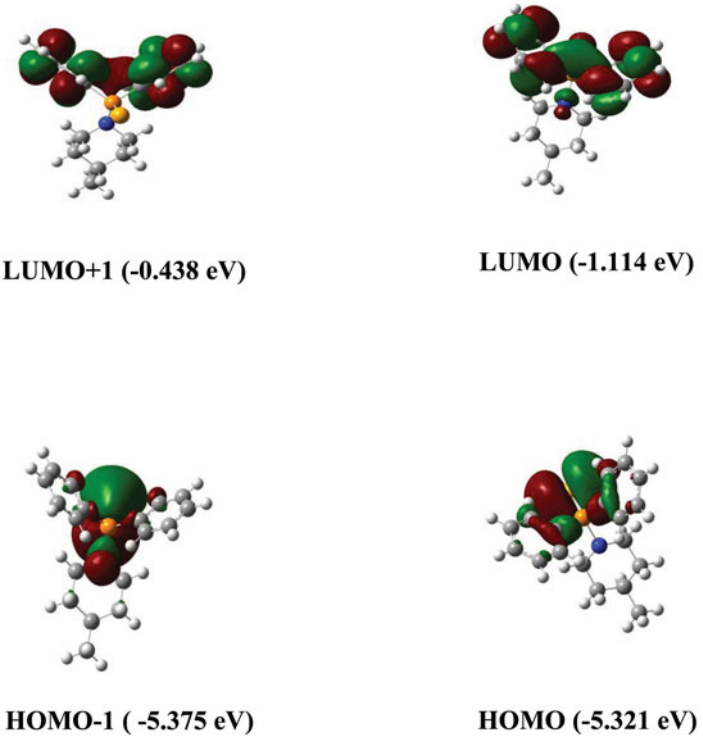

Figure 4. Molecular orbital surfaces and energy levels given in parentheses for the HOMO-1, HOMO, LUMO, and LUMO+1 of the title compound (1) computed at B3LYP/6-31G(*d*) level.

from the incident fields [36]. NLO is at the forefront of current research because of its importance in providing the key functions of frequency shifting, optical modulation, optical switching, optical logic, and optical memory for the emerging technologies in areas such as telecommunications, signal processing, and optical interconnections [37–40].

The NLO response of an isolated molecule in an electric field $E_i(\omega)$ can be presented as a Taylor series expansion of the total dipole moment, μ_{tot}, induced by the field:

$$\mu_{\text{tot}} = \mu_o + \alpha_{ij} E_j + \beta_{ijk} E_j E_k + \dots , \tag{2}$$

where α_{ij} is the linear polarizability, μ_o is the permanent dipole moment, and β_{ijk} are the first hyperpolarizability tensor components. The isotropic (or average) linear polarizability is defined as [41]:

$$\alpha_{\text{tot}} = \frac{\alpha_{xx} + \alpha_{yy} + \alpha_{zz}}{3} \tag{3}$$

First hyperpolarizability is a third rank tensor that can be described by $3 \times 3 \times 3$ matrix. The 27 components of 3D matrix can be reduced be to 10 components due to the Kleinman symmetry [42] ($\beta_{xyy} = \beta_{yxy} = \beta_{yyx}$, $\beta_{yyz} = \beta_{yzy} = \beta_{zyy}$; · likewise other permutations also take same value). The output from Gaussian 03 provides 10 components of this matrix as β_{xxx}, β_{xxy}, β_{xyy}, β_{yyy}, β_{xxz}, β_{xyz}, β_{yyz}, β_{xzz}, β_{yzz}, β_{zzz}, respectively. The components of the

first hyperpolarizability can be calculated using the following equation [41]:

$$\beta_i = \beta_{iii} + \frac{1}{3}\sum_{i\neq j}(\beta_{ijj} + \beta_{jij} + \beta_{jji}) \tag{4}$$

Using the x, y, and z components of β, the magnitude of the first hyperpolarizability tensor can be calculated by:

$$\beta_{\text{tot}} = \sqrt{(\beta_x^2 + \beta_y^2 + \beta_z^2)} \tag{5}$$

The complete equation for calculating the magnitude of β from Gaussian 03W output is given as follows:

$$\beta_{\text{tot}} = \sqrt{(\beta_{xxx} + \beta_{xyy} + \beta_{xzz})^2 + (\beta_{yyy} + \beta_{yzz} + \beta_{yxx})^2 + (\beta_{zzz} + \beta_{zxx} + \beta_{zyy})^2} \tag{6}$$

The calculations of the total molecular dipole moment (μ), linear polarizability (α), and first-order hyperpolarizability (β) from the Gaussian output have been explained in detail previously [43], and DFT has been extensively used as an effective method to investigate the organic NLO materials [44]. The electronic dipole moment μ_i ($i = x, y, z$), polarizability α_{ij} and the first hyperpolarizability β_{ijk} of the title compound were calculated at the B3LYP/6-31G(d) level using Gaussian 03W program package and listed in Table 6.

The calculated values of μ_{tot}, α_{tot}, and β_{tot} for the title compound are 1.708 D, 34.651 Å^3, and 1.399×10^{-30} cm^5 esu^{-1}, which are greater than those of urea (the μ_{tot}, α_{tot}, and β_{tot} of urea are 1.373 D, 3.831 Å^3, and 0.37289×10^{-30} cm^5 esu^{-1} obtained by B3LYP/6-31G(d) method) [36]. The title molecule shows a deviation from the planarity due to the steric interactions of protons of methyl and phenyl rings. The lack of planarity of the title molecule may be due to the free rotation of 4-methylpiperidine ring. Two phenyl rings of the molecule (I) are connected with selenium atom through two intramolecular hydrogen bonds, which will eventually stop the free rotation. When it is compared with the similar double bond compounds in literature, the calculated value of β_{tot} of (I) is smaller than that of 4-(2,3,4-trihydroxybenzylideneamino) antipyrine ($\beta_{\text{tot}} = 10.0125 \times 10^{-30}$ cm^5 esu^{-1}) [36] and 4-(2,3-dichlorobenzylideneamino) antipyrine ($\beta_{\text{tot}} = 25.191 \times 10^{-30}$ cm^5 esu^{-1}) [45] calculated with B3LYP/6-31G(d) method. Therefore, the title compound is a good candidate as a second-order NLO material.

Table 6. The calculated dipole moments (Debye), static polarizability components (a.u.) and first hyperpolarizability components (a.u.) for the title compound (1)

μ_x	0.3620	β_{xxx}	22.7297
μ_y	0.0001	β_{xxy}	0.0471
μ_z	−1.6693	β_{xyy}	11.1246
		β_{yyy}	−0.1746
α_{xx}	223.2985	β_{xxz}	69.8768
α_{xy}	0.0089	β_{xyz}	0.0220
α_{yy}	244.6856	β_{yyz}	−2.7970
α_{xz}	−12.4008	β_{xzz}	−11.7573
α_{yz}	−0.0288	β_{yzz}	0.0438
α_{zz}	233.4562	β_{zzz}	−227.5240

Many research works have indicated that the FMOs have significant effect on material NLO properties [43,46–49]. In quest of the NLO characteristics, the surfaces of FMOs of the studied molecules were investigated and shown in Fig. 4. We can see that the FMOs are mainly composed of atomic p-electron orbitals. It is evident that the NLO properties of the compounds are caused by the charge-transferring characteristics of FMOs of the molecules. However, the correlation between the first hyperpolarizabilities and energy gaps of HOMO–LUMO of the studied molecules are not following with the empirically inverse relationship reported previously [43, 48, 49].

Conclusions

In this work, the title compound (1) has been characterized by elemental analysis, ^{1}H NMR, ^{31}P NMR, X-ray analysis, and FT-IR techniques. Crystal packing of the title compound (1) is mainly dominated by intermolecular $C-H\cdot\pi$ hydrogen bonds formed during preparation or crystallization. Although it is well known that DFT-optimized bond lengths are usually longer and more accurate than HF because of the inclusion of electron correlation, the HF method correlates better for the bond length than the DFT method according to our calculations. However, the DFT method seems to be more appropriate than the HF method for obtaining the bond angles. The calculated results show that the optimized geometries can well reproduce the crystal structure, and the theoretical vibrational frequencies and chemical shift values. The MEP map shows that the negative potential site is on electronegative atom while the positive potential sites are around the hydrogen atoms. These sites give information about the region from where the compound can undergo intra- and intermolecular interactions. The predicted NLO properties of the title compound (1) are greater than those of urea. The title compound is a good candidate as a second-order NLO material.

As a result, all of these calculations will be provide helpful information to further studies on the title compound. Also, such response data will allow us to test different model approaches and explore the reliability of predictions.

A truly rational design and evaluation of novel catalysts remain out of reach, but we are optimistic that improving the description of ligand properties will prove vital for the interpretation and prediction of ligand effects on a broad range of catalytic reactions and that such insights can contribute to the development of novel catalysts. In addition, structure-activity relationship of the aminophosphine and derivatives can be investigated to make accurate and reliable predictions of the biological activity of new compounds and to facilitate the design and development of more effective drugs.

Acknowledgments

This study was financially supported by the Research Centre of Ondokuz Mayıs University (Project No: F-425) and TUBITAK (Project no: 110T572).

References

[1] Gopalakrishnan, J., & Rao, M. N. S. (2010). *Phosphorus, Sulfur Silicon Relat. Elem.*, *185*, 754.
[2] Al-Masri, H. T., Emwas, A.-H. M., Al-Talla, Z. A., & Alkordi, M. H. (2012). *Phosphorus, Sulfur Silicon Relat. Elem.*, *187*, 1082.
[3] Gopalakrishnan, J. (2009). *Appl. Organometal. Chem.*, *23*, 291.

[4] Zubiri, M. R., Milton, H. L., Slawin, A. M. Z., & Woollins, J. D. (2004). *Inorg. Chim. Acta*, *357*, 1243.
[5] Dixon, I. M., Lebon, E., Loustau, G., Sutra, P., Vendier, L., Igau, A., & Juris, A. (2008). *Dalton Trans.*, *41*, 5627.
[6] Bichler, B., Veiros, L. F., Öztopcu, Ö., Puchberger, M., Mereiter, K., Matsubara, K., & Kirchner, K. A. (2011). *Organometallics*, *30*, 5928.
[7] Sarıöz, Ö., Öznergiz, S., Saraçoğlu, H., & Büyükgüngör, O. (2011). *Heteroat. Chem.*, *22*, 679.
[8] Sarıöz, Ö., & Öznergiz, S. (2012). *Phosphorus, Sulfur Silicon Relat. Elem.*, *187*, 906.
[9] Burrows, A. D., Kociok-Köhn, G., Mahon, M. F., & Varrone, M. C. R. (2006). *Chimie*, *9*, 111.
[10] Sheldrick, G. M. (1997). *SHELXS-97 & SHELXL-97*, University of Gottingen: Germany.
[11] Scott, A. P., & Radom, L. (1996). *J. Phys. Chem.*, *100*, 16502.
[12] Ditchfield, R. (1972). *J. Chem. Phys.*, *56*(11), 5688.
[13] Wolinski, K., Hinton, J. F., & Pulay, P. (1990). *J. Am. Chem. Soc.*, *112*(23), 8251.
[14] Rauhut, G., Puyear, S., Wolinski, K., & Pulay, P. (1996). *J. Phys. Chem.*, *100*, 6310.
[15] Politzer, P., & Murray, J. S. (2002). *Theor. Chem. Acc. 108*, 134.
[16] Dennington, R. I. I., Keith, T., & Millam, J. (2007). *GaussView*, Version 4.1.2, Semichem, Inc.: Shawnee Mission, KS.
[17] Frisch, M. J., Trucks, G. W., Schlegel, H. B., Scuseria, G. E., Robb, M. A., Cheeseman, J. R., Montgomery Jr., J. A., Vreven, T., Kudin, K. N., Burant, J. C., Millam, J. M., Iyengar, S. S., Tomasi, J., Barone, V., Mennucci, B., Cossi, M., Scalmani, G., Rega, N., Petersson, G. A., Nakatsuji, H., Hada, M., Ehara, M., Toyota, K., Fukuda, R., Hasegawa, J., Ishida, M., Nakajima, T., Honda, Y., Kitao, O., Nakai, H., Klene, M., Li, X., Knox, J. E., Hratchian, H. P., Cross, J. B., Bakken, V., Adamo, C., Jaramillo, J., Gomperts, R., Stratmann, R. E., Yazyev, O., Austin, A. J., Cammi, R., Pomelli, C., Ochterski, J. W., Ayala, P. Y., Morokuma, K., Voth, G. A., Salvador, P., Dannenberg, J. J., Zakrzewski, V. G., Dapprich, S., Daniels, A. D., Strain, M. C., Farkas, O., Malick, D. K., Rabuck, A. D., Raghavachari, K., Foresman, J. B., Ortiz, J. V., Cui, Q., Baboul, A. G., Clifford, S., Cioslowski, J., Stefanov, B. B., Liu, G., Liashenko, A., Piskorz, P., Komaromi, I., Martin, R. L., Fox, D. J., Keith, T., Al-Laham, M. A., Peng, C. Y., Nanayakkara, A., Challacombe, M., Gill, P. M. W., Johnson, B., Chen, W., Wong, M. W., Gonzalez, C., & Pople, J. A. (2004). *Gaussian 03*; Revision E.01. Gaussian Inc.: Wallingford, CT.
[18] Farrugia, L. J. (1997). *J. Appl. Crystallogr.*, *30*, 565.
[19] Corbridge, D. E. C. (1995). *Phosphorus: An Outline of its Chemistry, Biochemistry and Uses*, Elsevier: Amsterdam.
[20] Song, X., & Bochmann, M. (1997). *J. Chem. Soc. Dalton Trans.*, *15*, 2689.
[21] Bochmann, M., Bwembya, G. C., Whilton, N., Song, X., Hursthouse, M. B., Coles, S. J., & Karaulov, A. (1995). *J. Chem. Soc. Dalton Trans.*, *11*, 1887.
[22] Bochmann, M., Bwembya, G. C., Hursthouse, M. B., Coles, S. J. (1995). *J. Chem. Soc. Dalton Trans.*, *17*, 2813.
[23] Cremer, D., & Pople, J. A. (1975). *J. Am. Chem. Soc.*, *97*, 1354.
[24] Bernstein, J., Davis, R. E., Shimoni, L., & Chang, N. L. (1995). *Angew. Chem. Int. Ed. Engl.*, *34*, 1555.
[25] Rastogi, V. K., Palafox, M. A., Tanwar, R. P., & Mittal, L. (2002). *Spectrochim. Acta*, *A58*, 1987.
[26] Silverstein, M., Basseler, G. C., & Morill, C. (1981). *Spectrometric Identification of Organic Compounds*, Wiley: New York.
[27] Biricik, N., Durap, F., & Gümgüm, B. (2007). *Transition Met. Chem.*, *32*, 877.
[28] Demir, S., Dinçer, M., Korkusuz, E., & Yıldırım, İ. (2010). *J. Mol. Struct.*, *980*, 1.
[29] Scrocco, E., & Tomasi, J. (1978). *Adv. Quant. Chem.*, *11*, 115.
[30] Luque, F. J., Lopez, J. M., & Orozco, M. (2000). *Theor. Chem. Acc.*, *103*, 343.
[31] Okulik, N., & Jubert, A. H. (2005). *Internet. Electron J. Mol. Des.*, *4*, 17.
[32] Politzer, P., Laurence, P. R., & Jayasuriya, K. (1985). *Environ. Health Perspect.*, *61*, 191.
[33] Scrocco, E., & Tomasi, J. (1973). *Top. Curr. Chem.*, *7*, 95.

[34] Politzer, P., & Truhlar, D. G. (1981). *Chemical Applications of Atomic and Molecular Electrostatic Potentials*, Plenum Press: New York.
[35] Fleming, I. (1976). *Frontier Orbitals and Organic Chemical Reactions*, Wiley: London.
[36] Sun, Y. X., Hao, Q. L., Wei, W. X., Yu, Z. X., Lu, L. D., Wang, X., & Wang, Y. S. (2009). *J. Mol. Struct. Theochem.*, *904*, 74.
[37] Andraud, C., Brotin, T., Garcia, C., Pelle, F., Goldner, P., Bigot, B., & Collet, A. (1994). *J. Am. Chem. Soc.*, *116*, 2094.
[38] Geskin, V. M., Lambert, C., & Bredas, J. L. (2003). *J. Am. Chem. Soc.*, *125*, 15651.
[39] Nakano, M., Fujita, H., Takahata, M., & Yamaguchi, K. (2002). *J. Am. Chem. Soc.*, *124*, 9648.
[40] Sajan, D., Joe, H., Jayakumar, V. S., & Zaleski, J. (2006). *J. Mol. Struct.*, *785*, 43.
[41] Zhang, R., Du, B., Sun, G., & Sun, Y. X. (2010). *Spectrochim. Acta*, *A75*, 1115.
[42] Kleinman, D. A. (1962). *Phys. Rev.*, *126*, 1977.
[43] Thanthiriwatte, K. S., & Nalin de Silva, K. M. (2002). *J. Mol. Struct. Theochem.*, *617*, 169.
[44] Sun, Y. X., Hao, Q. L., Yu, Z. X., Wei, W. X., Lu, L. D., & Wang, X. (2009). *Mol. Phys.*, *107*, 223.
[45] Sun, Y. X., Hao, Q. L., Wei, W. X., Yu, Z. X., Lu, L. D., Wang, X., & Wang, Y. S. (2009). *J. Mol. Struct. 929*, 10.
[46] Liyanage, P. S., de Silva, R. M., & de Silva, K. M. N. (2003). *J. Mol. Struct. (Theochem)*, *639*, 195.
[47] Li, F.-F., Wu, D.-S., Lan, Y.-Z., Shen, J., Huang, S.-P., Cheng, W.-D., Zhang, H., & Gong, Y.-J. (2006). *Polymer*, *47*, 1749.
[48] Oberg, K., Berglund, A., Edlund, U., & Eliasson, B. (2001). *J. Chem. Inf. Comput. Sci.*, *41*, 811.
[49] Zheng, W., Wong, N.-B., Li, W. K., & Tian, A. (2006). *J. Chem. Theory Comput.*, *2*(3), 808.